

## Lecture 11

### Fractional Melting

Somewhat analogous to fractional crystallization there is a process of fractional melting, but in fact with respect to solid state diffusion, these two fractional models are quite distinct (Figure 33).

#### Surface Equilibrium Models

Fractional Crystallization:	Fractional Melting:
1) homogeneous liquid at all time	1) homogeneous solid at all times. Note this requires that solid state diffusion enables equilibrium
2) cool	2) melt
3) precipitate crystals whose surface is in equilibrium with liquid but whose interiors are removed from equilibration; i.e. solid state diffusion is slow relative to crystal growth rate.	3) infinitesimal increments of melt are formed in equilibrium with the entire residual solid. However, each melt increment is instantaneously removed from the system after it is formed. Thus this model requires efficient segregation of melt from the residue. <u>In its pure form this model is not realistic because it requires rapid solid state diffusion.</u> Note how this model differs from batch melting, where melt does not segregate until F equals a particular value. An important issue is the physics of melt segregation.
4) equations <u>basic assumption</u> $\frac{dx_s}{dM_s} = D \frac{x_\ell}{M_\ell}$ leads to $C_\ell / C_o = F^{D-1}$ $C_s^{\text{instant}} / C_o = D(F)^{D-1}$ $\bar{C}_s^{\text{avg}} / C_o = \frac{1-F^D}{1-F}$ where $F = \text{melt fraction}$	4) equations <u>basic assumption</u> $\frac{dx_\ell}{dM_\ell} = D \frac{x_s}{M_s}$ leads to $C_s / C_o = (1-F)^{\frac{1}{D}} - 1$ $C_\ell^{\text{instant}} / C_o = \frac{1}{D} (1-F)^{\frac{1}{D}-1}$ $\bar{C}_\ell^{\text{avg}} / C_o = \frac{1-(1-F)^{1/D}}{F}$
5) petrologic process is segregation of zoned crystals from melt, creating a residual melt composition	5) petrologic process is segregation and eruption of instantaneous melts or mixing of instantaneous melts in a magma chamber

Figure 33. The concepts, assumptions and simple equations for the processes of Fractional Crystallization and Fractional Melting.

There are two end-member melts arising from fractional melting: (a) instantaneous fractional melts which become very depleted in abundances of highly incompatible elements as melting proceeds, i.e.  $\frac{C^L}{C^O} \ll 1$ ; (b) average or accumulated fractional melt which is quite similar to equilibrium melts, commonly described as “batch melts” (Figure 34).

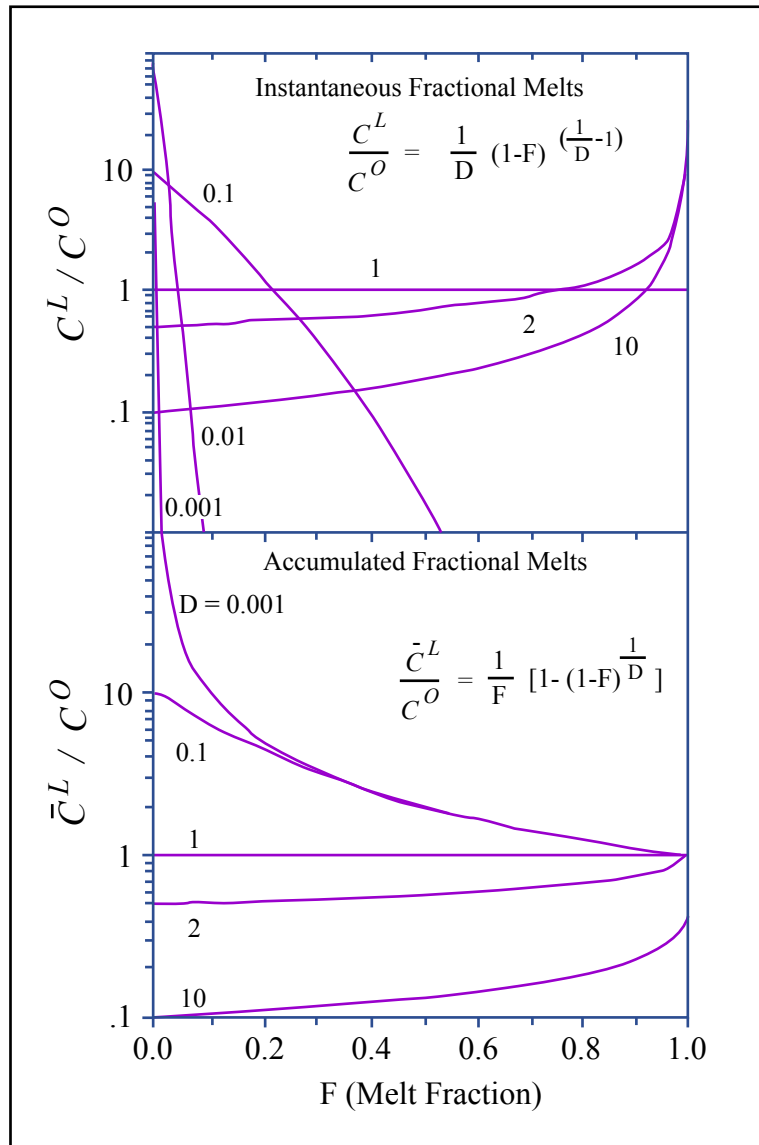


Figure by MIT OpenCourseWare.

Figure 34. Concentrations of trace elements with  $D = 0.001$  to  $10$  in melts created by modal fractional melting ( $C^L$ ) relative to unmelted source abundance ( $C^O$ ). Upper: fractional, i.e., instantaneous, melts created at a given  $F$ . Lower: Instantaneous melts are accumulated, e.g., in a magma chamber and mixed to form an average melt.

As previously discussed, Shaw (1970, GCA) developed equations for non-modal melting using

$$D = \frac{D_o - PF}{1 - F} \text{ where } P = D^{\alpha/\ell} p^\alpha + D^{\beta/\ell} p^\beta \text{ with } p^j = \text{proportion of phase "j" in melt, and}$$

$$\sum p^j = 1.$$

Then, the modal melting equation

becomes for non-modal melting

<u>Batch melts:</u> $C^\ell / C^o = \frac{1}{D_o + F(1 - D_o)}$ (Shaw Eqn. 11)	$C^\ell / C^o = \frac{1}{D_o + F(1 - P)}$ (Shaw Eqn. 15)
<u>Residues:</u> $C^s / C^o = \frac{D_o}{D_o + F(1 - D_o)}$	$C^s / C^o = \left(\frac{D_o - PF}{1 - F}\right) \left(\frac{1}{D_o + F(1 - P)}\right)$

Similarly for fractional melting

<u>modal melting</u>	<u>non-modal melting</u>
<u>Aggregated melts:</u> $\bar{C}^\ell / C^o = \frac{1 - (1 - F)^{1/D_o}}{F}$ (Shaw Eqn. 10)	$\bar{C}^\ell / C^o = \frac{1}{F} \left[1 - \left(1 - \frac{PF}{D_o}\right)^{\frac{1}{P}}\right]$ (Shaw Eqn. 14)
<u>Residues:</u> $C^s / C^o = (1 - F)^{\frac{1}{D_o} - 1}$ (Shaw Eqn. 9)	$C^s / C^o = \frac{1}{1 - F} \left(1 - \frac{PF}{D_o}\right)^{\frac{1}{P}}$ (Shaw Eqn. 16)
<u>Instantaneous melts:</u> $C^\ell / C^o = \frac{1}{D_o} (1 - F)^{\frac{1}{D_o} - 1}$ (Shaw Eqn. 8)	$C^\ell / C^o = \frac{1}{D_o} \left(1 - \frac{PF}{D_o}\right)^{\left(\frac{1}{P} - 1\right)}$ (Shaw Eqn. 13)

It is important to compare the trace element contents of partial melts and residual solids formed by batch and fractional melting in particular, both instantaneous and average or accumulated fractional melts. This is readily accomplished by calculations for a simple model for non-modal melting of a garnet pyroxenite (Figure 35). The calculated results are shown in Figure 36. Most notable is that during fractional melting as F increases the incompatible element content of the residue becomes very low; consequently, the instantaneous melt derived from residue created at high F (>0.05) has very low concentration of incompatible elements.

### **Non-modal melting of olivine-bearing garnet pyroxenite**

<u>Mineralogy</u>	<u>Initial Proportion</u>	<u>D<sub>La</sub><sup>mineral/melt</sup></u>	<u>melt proportion (p)</u>
olivine	0.3	0.008	0
orthopyroxene	0.2	0.01	0
clinopyroxene	0.3	0.08	0.5
garnet	0.2	0.02	0.5

### **Results for batch and fractional melting**

F	c <sup>l</sup>	$\bar{C}^l$	c <sup>s</sup>	c <sup>L</sup>	c <sup>S</sup>
0.001	39.0	39.5	1.3	39.0	1.3
0.01	30.0	34.8	0.96	31.0	1.0
0.1	1.7	12.5	0.051	10.2	0.31
0.2	0.036	6.5	0.001	5.8	0.16
0.64	0	2.0	0	2.0	0.002

where  $C_i^0 = 1.3 \text{ ppm}$ ,  $D_o^{\text{bulk solid/melt}} = 0.0324$ .  $C^l$  and  $\bar{C}^l$  are instantaneous and average fractional melts,  $C^s$  is residue of fractional melting,  $C^L$  and  $C^S$  are batch melts and residual solids formed by equilibrium melting.

Figure 35. Upper: Non-modal melting model for garnet pyroxenite indicating initial phase proportions, partition coefficients for a highly incompatible element such as La and proportions of phases contributing to the melt.  
Lower: Calculated results for melts and solids created by fractional and batch melting using equations in text (Shaw, 1970). Example is modified from Shaw (1978).

Since fractional melting assumes that solid state diffusion is rapid relative to melt segregation, a more realistic approximation for partial melting is incremental melting where the number of melt increments is intermediate between 1 (batch melting) and infinity (fractional melting). Moreover, a useful way to gain an understanding of the extreme incompatible element depletion that is characteristic of instantaneous fractional melts (Figures 34 and 36) is to consider the melting process as a series of steps or increments. In step 1 the source transfers most of its inventory of incompatible elements to melt increment 1 thereby creating residue 1 which is relatively depleted in incompatible elements, i.e.  $C^s/C^o < 1$ . Then the process continues with the step 2 melt forming from its source which is the residue formed in step 1. In other words the source of each incremental melt is the residue formed during the previous step. It is important to realize that at each melting step, the entire residue equilibrates with the incremental melt; i.e., the residual solid is homogeneous and at each step equilibrium partitioning occurs, i.e.  $D^{\text{residual solid/fractional melt}}$  is in effect. Hence as the number of melting steps increases the source of the next melt increment is more strongly depleted in incompatible elements as clearly seen for  $C^l/C^o$  as  $F > 0.01$  in Figures 34 and 36.

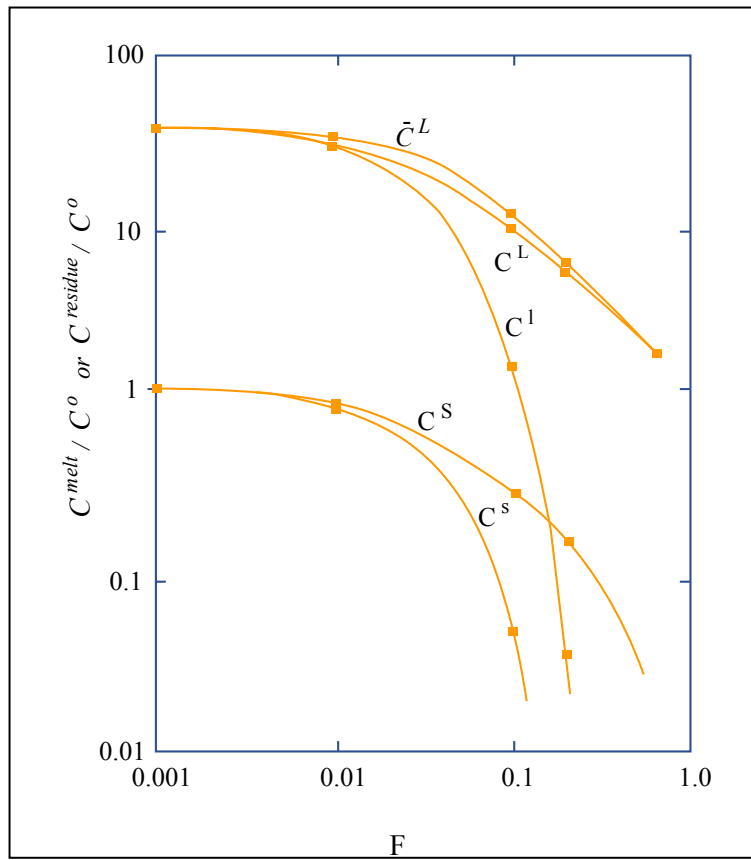


Figure by MIT OpenCourseWare.

Figure 36. Plots of calculated results shown in Figure 35. Important points are:

- (a) Batch melts ( $C^L$ ) and average (aggregated) melts from fractional melting ( $\bar{C}^l$ ) are quite similar, approaching  $1/D$  at low  $F$  and  $C_1^o$  at high  $F$ .
- (b) In contrast the instantaneous melt ( $C^l$ ) created by fractional melting is depleted in the incompatible element relative the source content as  $F$  exceeds 0.01.
- (c) The residue from fractional melting ( $C^s$ ) is highly depleted in the incompatible element as  $F$  exceeds 0.05.

Figure is modified from Shaw (1978).

The example shown in Figures 35 and 36 assumes a constant mineral/melt partition coefficient (D). Hertogen and Gijbels (1978) considered a more complex model of linearly increasing or decreasing D as F increases. The input parameters are in Figure 37 and Figure 38 shows a comparison of results for batch and average fractional melts.

Melting model for a lherzolite with initial modal proportions of ol: 50%, opx: 30%, cpx: 20%.

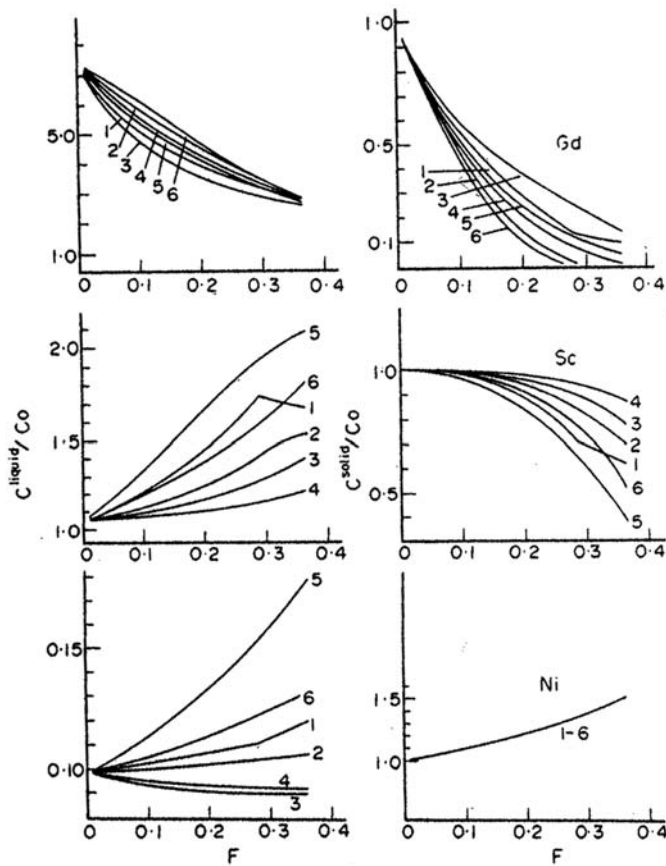
	Model A			Model B			Model C		
	Constant partition coefficients and melting proportions.			Linearly increasing partition coefficients and varying p.			Linearly decreasing partition coefficients, and varying p.		
	Ol	Opx	Cpx	Ol	Opx	Cpx	Ol	Opx	Cpx
D <sup>Gd</sup>	0.010	0.10	0.50	0.010 0.015	0.10 0.15	0.50 (F=0) 0.75 (F=0.364)	0.010 0.005	0.10 0.05	0.50 0.25
D <sup>Sc</sup>	0.1	1.	3.	0.10 0.15	1.0 1.5	3. 4.	0.10 0.05	1.0 0.5	3. 2.
D <sup>Ni</sup>	15.	6.5	3.5	15. 20.	6.5 9.0	3.5 5.0	15. 10.	6.5 4.0	3.5 2.0
p	0.1 (F = 0 → 0.286)	0.2	0.7	0.1 0.2	0.2 0.4	0.7 (F=0) 0.4 (F=0.364)	as in model B		
p	0.33 (F = 0.286 → 0.364)	0.67							

\*ol = olivine; opx = orthopyroxene; cpx = clinopyroxene.

Model A is a two step process, as clinopyroxene is used up at 28.6% melting. In Models B and C the partition coefficients and melting proportions linearly vary between the two extreme values for F = 0 and F = 0.364, i.e. at the disappearance of clinopyroxene. For the three models the modal composition of the residual solid at F = 0.364 is 70% olivine and 30% orthopyroxene.

Figure 37. Input parameters for melting models of lherzolite with varying  $D_{\text{mineral}/\text{melt}}$  and mineral proportions ( $p_j$ ) entering the melt. Modified from Hertogen and Gijbels (1976).

A summary of significant results for each element follows (Figure 38).



Courtesy of Elsevier, Inc., <http://www.sciencedirect.com>. Used with permission.

Figure 38. Relative concentration of Gd, Sc and Ni in the liquid and residual solid, produced by non-modal melting of a lherzolite assemblage;  $C^{\text{liquid}}/C_0$  stands for  $\bar{C}^{\text{L}}/C_0$  or  $C^{\text{L}}/C_0$ ; that is, in all cases the fractional melt curves are for the average or aggregated fractional melt. Curve 1: model A, batch melting, 2: model A, fractional melting, 3: model B, batch melting, 4: model B, fractional melting 5: model C, batch melting, 6: model C, fractional melting (figure is from Hertogen and Gijbels, 1976).

Gd (a highly incompatible element): For the melt, models 1 to 6 are quite similar despite varying partition coefficients and phase proportions entering the melt. In contrast, the residual solids are more highly depleted in residues created by fractional melting (models 2, 4, 6).

Sc (a moderately incompatible element in olivine and orthopyroxene but compatible in clinopyroxene): Most surprising are the positive slopes for  $C^\ell/C^0$ ; this is an unanticipated result because as  $F \rightarrow 1$ ,  $C^\ell/C^0 = 1$ . What is the explanation? Note that  $D_0^{\text{bulk solid/melt}}$  for Sc is 0.95 but because clinopyroxene preferentially enters the melt ( $p^{\text{cpx}} = 0.70$ ) (Figure 37) the bulk solid/melt D for Sc initially decreases as F increases. Eventually as F increases the slope of  $C^\ell/C^0$  vs. F for Sc becomes negative; e.g. at  $F = 0.286$  for model 1 (Figure 38).

Ni (a highly compatible element):  $C_{\text{Ni}}^\ell/C_{\text{Ni}}^0$  is very sensitive to increasing  $D_{\text{Ni}}^{s/\ell}$  (model 3) or decreasing  $D_{\text{Ni}}^{s/\ell}$  (model 5). Note that the slopes are nearly horizontal for models 2, 3 and 4 showing that for these cases  $D_{\text{Ni}}^{s/\ell}$  is insensitive to F. Since only a small proportion of the Ni inventory resides in the partial melts, at the scales shown for  $C_{\text{Ni}}^s/C_{\text{Ni}}^0$  all models plot along the same trajectory.

MIT OpenCourseWare  
<http://ocw.mit.edu>

**12.479 Trace-Element Geochemistry**

Spring 2013

For information about citing these materials or our Terms of Use, visit: <http://ocw.mit.edu/terms>.